The American Journal of Human Genetics, Volume *104*

Supplemental Data

Mutations in *NCAPG2* Cause a Severe Neurodevelopmental Syndrome that Expands the Phenotypic Spectrum of Condensinopathies

Tahir N. Khan, Kamal Khan, Azita Sadeghpour, Hannah Reynolds, Yezmin Perilla, Marie T. McDonald, William B. Gallentine, Shahid M. Baig, Task Force for Neonatal Genomics, Erica E. Davis, and Nicholas Katsanis

Supplementary Information

Supplemental Note

Task Force for Neonatal Genomics Consortium

Alexander Allori[7], Misha Angrist[8], Patricia Ashley[9], Margarita Bidegain[9], Brita Boyd[10], Eileen Chambers[11], Heidi Cope[1,12], C. Michael Cotten[9], Theresa Curington[1], Erica E. Davis[1], Sarah Ellestad[10], Kimberley Fisher[13], Amanda French[14], William Gallentine[5], Ronald Goldberg[9], Kevin Hill[15], Sujay Kansagra[5], Nicholas Katsanis[1], Sara Katsanis[8], Joanne Kurtzberg[16], Jeffrey Marcus[7], Marie McDonald[4], Mohammed Mikati[5], Stephen Miller[15], Amy Murtha[10], Yezmin Perilla[1], Carolyn Pizoli[5], Todd Purves[17], Sherry Ross[17,18], Azita Sadeghpour[1], Edward Smith[5], John Wiener[17]

[1]Center for Human Disease Modeling, Duke University Medical Center, Durham, NC USA
[4]Department of Pediatrics, Division of Medical Genetics, Duke University Medical Center, Durham, NC USA
[5]Department of Pediatrics, Division of Pediatric Neurology, Duke University Medical Center, Durham, NC USA
[7]Department of Surgery, Division of Plastic Maxillofacial and Oral Surgery, Duke University Medical Center, Durham, NC USA
[8]Science and Society, Duke University School of Medicine, Durham, NC USA
[9]Department of Pediatrics, Division of Neonatology, Duke University Medical Center, Durham, NC USA
[10]Department of Obstetrics and Gynecology, Division of Maternal-Fetal Medicine, Duke University Medical Center, Durham, NC USA
[11]Department of Pediatrics, Division of Pediatric Nephrology, Duke University Medical Center, Durham, NC USA
[12]Department of Medicine, Duke University Medical Center, Durham, NC, USA
[13]Neonatal Perinatal Research Unit, Duke University Medical Center, Durham, NC USA
[14]Fetal Diagnostic Center, Duke University Medical Center, Durham, NC USA
[15]Department of Pediatrics, Division of Pediatric Cardiology, Duke University Medical Center, Durham, NC USA
[16]Department of Pediatrics, Division of Pediatric Blood and Marrow Transplantation, Duke University Medical Center, Durham, NC USA
[17]Department of Surgery, Division of Pediatric Urology, Duke University Medical Center, Durham, NC USA
[18]Department of Urology, University of North Carolina, Chapel Hill, NC USA

Supplemental Case Report: Family 1

The female proband was born at 42 weeks via normal spontaneous vaginal delivery to a 37-year-old G3P3 mother and a 35-year-old father with no known contributory family history. The parents are of European ancestry (Ukrainian, Polish, German and English) and consanguinity was denied. The pregnancy was complicated by advanced maternal age (AMA), a maternal kidney infection in the first trimester and ultrasound findings. Prenatal ultrasound at 41 weeks revealed multiple fetal anomalies including frontal bossing; two-vessel cord; renal findings interpreted as a possible cyst or hydronephrosis; and dilated cerebral ventricles. The delivery was uncomplicated, and the Apgar score was 5 at 1 minute and 9 at 5 minutes. The birth weight, length and head circumference were 3463 grams (55th percentile), 48 cm (30th percentile) and 33.5 cm (22nd percentile), respectively. Upon physical examination at birth, she was found to have severe hypotonia, bilateral postaxial polydactyly on the feet, sacral dimple, weak cry, weak suck, and poorly coordinated swallow. During the first month of life, she developed febrile pyelonephritis and was diagnosed with bilateral grade IV vesicoureteral reflux.

During the neonatal period, developmental concerns were noted and have persisted through childhood. During the first few months of life, she did not roll over, had poor head control and also displayed head lag. She was eventually able to hold her head up at 12 months of age, sit without support at 3 ½ years, roll over at 3 ½ - 4 years, speak her first single word at 4 ½ years, and walk independently at 6 years. Currently at age 11, she has moderate intellectual disability, is non-verbal and uses limited sign language. Coincident with developmental delay, we noted a reduction in her growth parameters during infancy. On physical exam at 8 months of age, she had a height of 58.5 cm (<1st percentile), weight at 5.8 kg (<1st percentile) and head

circumference of 40.5 cm (1st percentile). Additionally, she presented with microcephaly with frontal bossing; open anterior fontanelle; a short nose with tented; triangular mouth; severe eczema of the skin; underdeveloped/absent clitoris; mild pectus excavatum; slightly abnormal introitus; and an abnormally placed anus.

The family 1 proband has undergone extensive clinical imaging and assessment of neurological, urogenital, ocular, auditory, and skeletal structure and/or function.

Central nervous system. An initial brain MRI at 6 months of age raised a concern for Joubert syndrome due to possible molar tooth sign. Subsequent review of MRI and a repeat MRI, at 22 months of age, did not support the presence of a molar tooth. However, the MRI did reveal mild volume loss, colpocephaly and cerebellar vermian hypoplasia (Figure 1B).

Urogenital findings. Renal ultrasound at 12 months of age revealed bilateral grade I hydronephrosis (Figure 1C). A fluoroscopy voiding urethrocystogram confirmed the bilateral vesicoureteral reflux. Her follow up imaging at 8 years of age continued to show hydronephrosis and bilateral vesicoureteral reflux. However, her last renal ultrasound at 10 years of age was normal except for a small right kidney (5.9 cm; average normal size for age is 8.5 cm). In addition, she has ureteral duplication.

Ocular phenotypes. During neonatal period, she was diagnosed with nystagmus and strabismus. An ophthalmology evaluation at 11 months of age demonstrated epiblepharon with entropion of both eyes, corneal scarring, absent tear duct on the right side, and pigmentary retinopathy. Currently at age 11, she has visual impairment due to retinal and optic nerve abnormalities.

Skeletal and digit abnormalities. An MRI of the spine at 14 months of age noted borderline position of conus medullaris at L3, a thickened filum, a tethered cord (repaired surgically at 15

months of age) and no evidence of scoliosis. A spine radiograph at 3 years of age showed a significant left thoracolumbar scoliosis. A follow up spine x-ray at 4 years of age revealed an S-shaped scoliosis (Figure 1E). She underwent surgical correction (Shilla technique) at 7 years of age and is currently doing well. Radiography of her feet at 19 months of age revealed 6 digits in each foot, each with a proximal, middle, and distal phalynx (Figure 1G). There are 5 metatarsals bilaterally. The fifth and sixth digits are centered at the fifth metatarsal heads. The fifth metatarsal heads likely have two separate articular surfaces. There is abnormal widening of the right first and second toe space.

Auditory function. Brainstem auditory evoked response (BAER) at 3 years of age revealed normal hearing bilaterally. A tympanoplasty was performed to repair the tympanic membrane perforation in her right ear. BAER at 8 years of age indicated a mild/minimal high frequency sensorineural hearing loss in the left ear and a mild/moderate sensorineural hearing loss in the right ear. She is currently using a hearing aid in the right ear.

At her last physical examination, she was below the 3rd centile for height (11 years; 116.8 cm). Additionally, she has extensive food allergies and is diagnosed with obstructive sleep apnea. This individual has three siblings who do not display any aspects of this complex phenotype, with the exception of a male sibling with short stature and a delayed bone age.

We performed karyotyping using cells from whole peripheral blood (n=20 cells), and observed a 46,XX karyotype with normal band length and morphology (Figure S1A). One cell (5%) displayed a break in two different chromosomes (11 and 13), but the clinical significance of this observation is unclear (Figure S1B). Chromosomal microarray (CMA) revealed an interstitial

deletion of ~153.7 kb on chromosome 2q13 which encompasses *NPHP1* (minimally deleted segment, chr2:110833630-110987359 [hg19]; CytoScan HD, Affymetrix). Deletion testing of *NPHP1* showed the variant to be a paternally inherited heterozygous aberration, and sequencing of the coding regions and splice junctions of *NPHP1* in a research laboratory were negative. We performed further candidate gene sequencing informed by proband phenotype; mutational screening of *AH11*, *CEP290*, *MKS3/TMEM67*, *MECP2*, and *ROR2* in a clinical laboratory yielded no diagnostic mutations. Further non-genetic diagnostic testing included monitoring of urine oligosaccharide and free glycan; results for both tests were within normal limits.

Supplemental Case Report: Family 2

The female proband was born at 34-weeks to a 39-year-old G3P4 mother and a 33-year-old father of Mexican ancestry. The family history is non-contributory, and consanguinity was denied but we note that both parents' families originate from the same region in Mexico. The pregnancy was complicated by AMA, twin gestation, and severe intra uterine growth restriction (IUGR) of the proband, or twin "B". Prenatal laboratory testing was unremarkable with the exception of Group B Strep (GBS) status unknown. Delivery was performed via C-section due to severe IUGR of twin "B" and breech presentation of twin "A". Amniotic fluid was meconium stained. Apgar scores were 6 at one minute, 7 at five minutes, and 9 upon repeat scoring. Her birth weight, length and head circumference were 0.84 kg (<1st percentile), 34 cm (<1st percentile) and 25 cm (<1st percentile), respectively.

Her neonatal course was complicated by prematurity, anemia, neutropenia, lymphopenia, failure to thrive and heart murmur. She underwent extensive clinical assessment to evaluate the structure and function of various organ systems:

Central nervous system and craniofacial features. She displayed severe microcephaly, and brain MRI at one month of age showed morphologically normal appearance of the brain. Furthermore, she displayed contractures of left arm and leg, neonatal hypertonia, and sacral dimple with low-lying conus medullaris without tethered cord (Figure 1F). Her facial features included micrognathia and arched eyebrows.

Urogenital findings. Renal ultrasound at two days of life revealed small but otherwise normal kidneys. The proband developed bilateral grade 2 hydronephrosis at 6 weeks of age (Figure 1D), which was resolved after 2 months.

Ocular phenotypes. Ophthalmology exam revealed bilateral opaque cornea consistent with Peters anomaly; bilateral congenital glaucoma; and buphthalmos of the left eye. At the age of 2 months the baby underwent multiple eye surgeries including optical iridectomy of right eye and trans-scleral diode laser cycloablation (TDC) of both eyes. She still had no vision in left eye.

Skeletal and digit abnormalities. We noted digit abnormalities at birth; these included absent 4^{th} and 5^{th} toes on the left foot and 5^{th} toe on right foot as well as clinodactyly of 5^{th} finger on right hand.

Auditory function. Newborn screening was normal. Initial newborn hearing screen of right ear failed. However, she passed hearing screen for both ears 6 weeks of age.

Cardiovascular. The newborn underwent echocardiography demonstrating a large patent ductus arteriosus, a large patent foramen ovale and a mild tricuspid regurgitation. Follow up imaging

revealed a bilateral superior vena cava with absent bridging vein but did not show a patent ductus arteriosus.

Barium swallow imaging revealed severe oropharyngeal dysphasia and therefore, at the age of 3 months, a gastric tube was placed. The proband was discharged stable after 4 months of hospitalization however, she passed away 4 days later. Autopsy was declined by the parents, and the cause of death is unknown. She is survived by three siblings, including her twin brother who has heart murmur and reactive airway disease. The other two siblings are reported to have no congenital malformations.

Fluorescence in situ hybridization (FISH) was normal and did not reveal aneuploidies for chromosomes 13, 15, 18, 21 and X. We were unable to obtain interpretable karyotype results due to a lack of mitotic activity. CMA revealed a female result with several independent regions showing absence of heterozygosity (AOH), encompassing approximately 3% of the genome, although the parents deny consanguinity. We tested a repeat peripheral blood specimen in a chromosome diepoxybutane (DEB) assay for Fanconi anemia, and did not detect chromosome breakage or rearrangements; the first peripheral blood specimen yielded uninterpretable results due to a lack of mitotic activity. Clinical sequence analysis and deletion testing of the mitochondrial genome did not identify any disease-causing mutations.

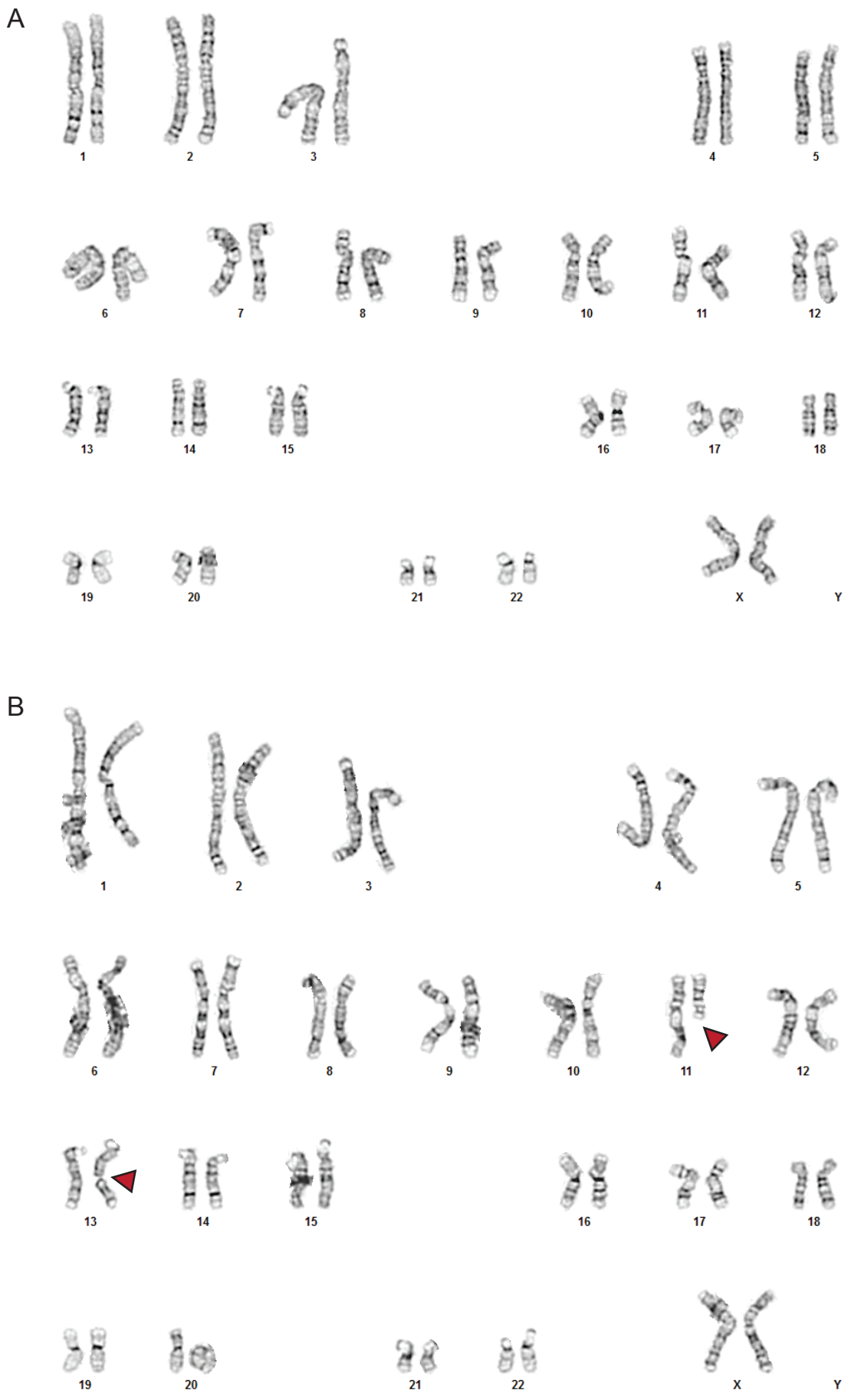
A
1
2
3
4
5
6
7
8
9
10
11
12
13
14
15
16
17
18
19
20
21
22
X
Y
B
1
2
3
4
5
6
7
8
9
10
11
12
13
14
15
16
17
18
19
20
21
22
X
Y

Figure S1

Figure S1. Representative karyograms from the family 1 proband.

(**A** and **B**) Cells from whole peripheral blood were fixed with 3:1 methanol/acetic acid, and GTW bands were visualized with Wright's stain at 550-650 band resolution. Chromosomes show normal band length and morphology (46,XX; n=20 cells). One cell (5%) displayed chromosome breaks on chromosome 11 and 13 (panel B; red arrowheads).

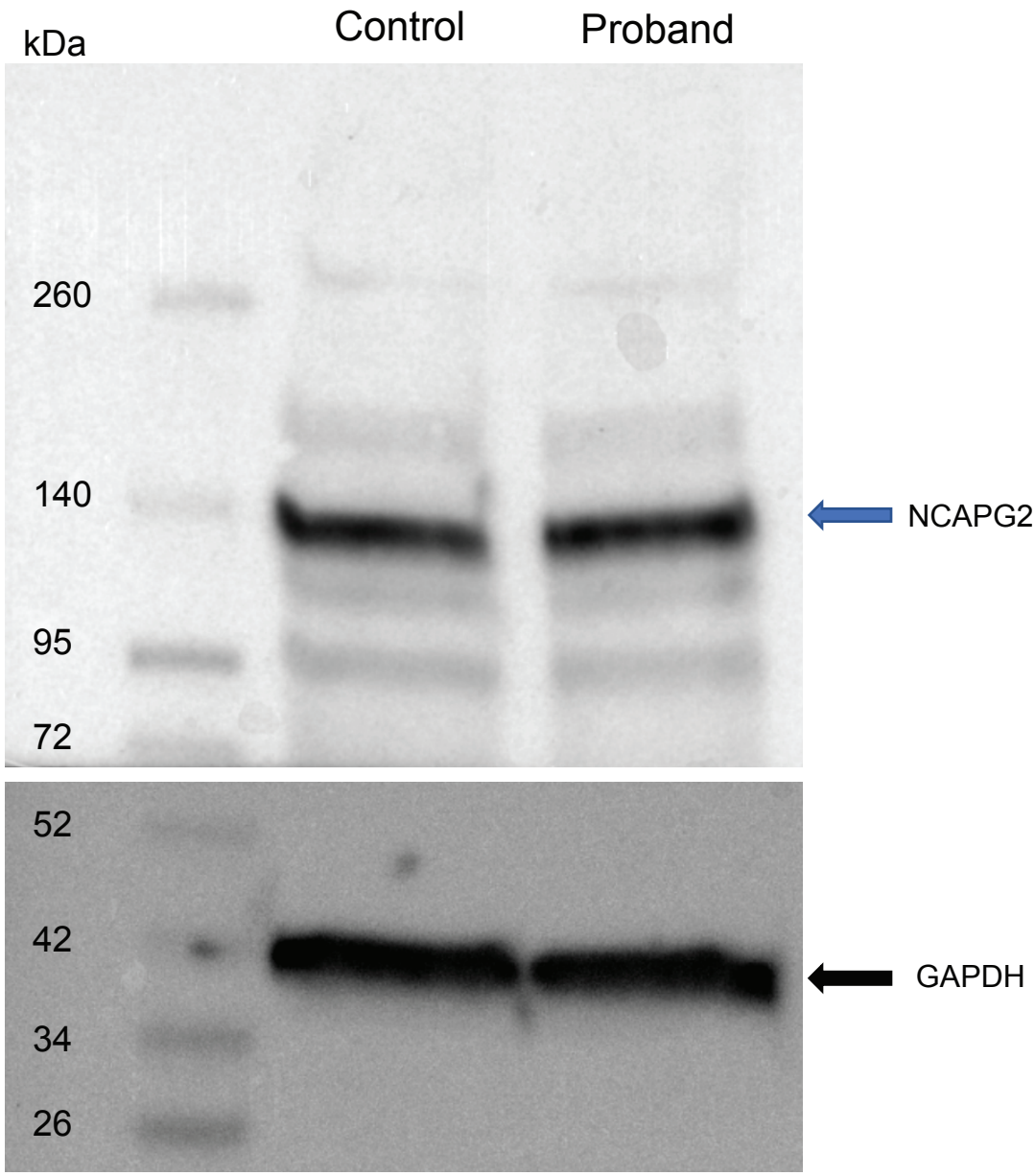

Figure S2

Figure S2. Immunoblotting of NCAPG2 on whole cell lysates from the family 1 proband lymphoblast cells showed no detectable reduction in NCAPG2 protein.

Western blot was performed on 50 μg whole-cell protein isolated from control and family 1 proband lymphocyte cell lines using rabbit anti-CAP-G2 antibody (Bethyl Laboratories, A300-605A-T; 1:1000 dilution). Blue arrow indicates NCAPG2 protein with predicted molecular weight of ~130 kDa; black arrow indicates GAPDH (Santa Cruz Biotechnology, SC-47727; 1:2000 dilution) as a loading control.

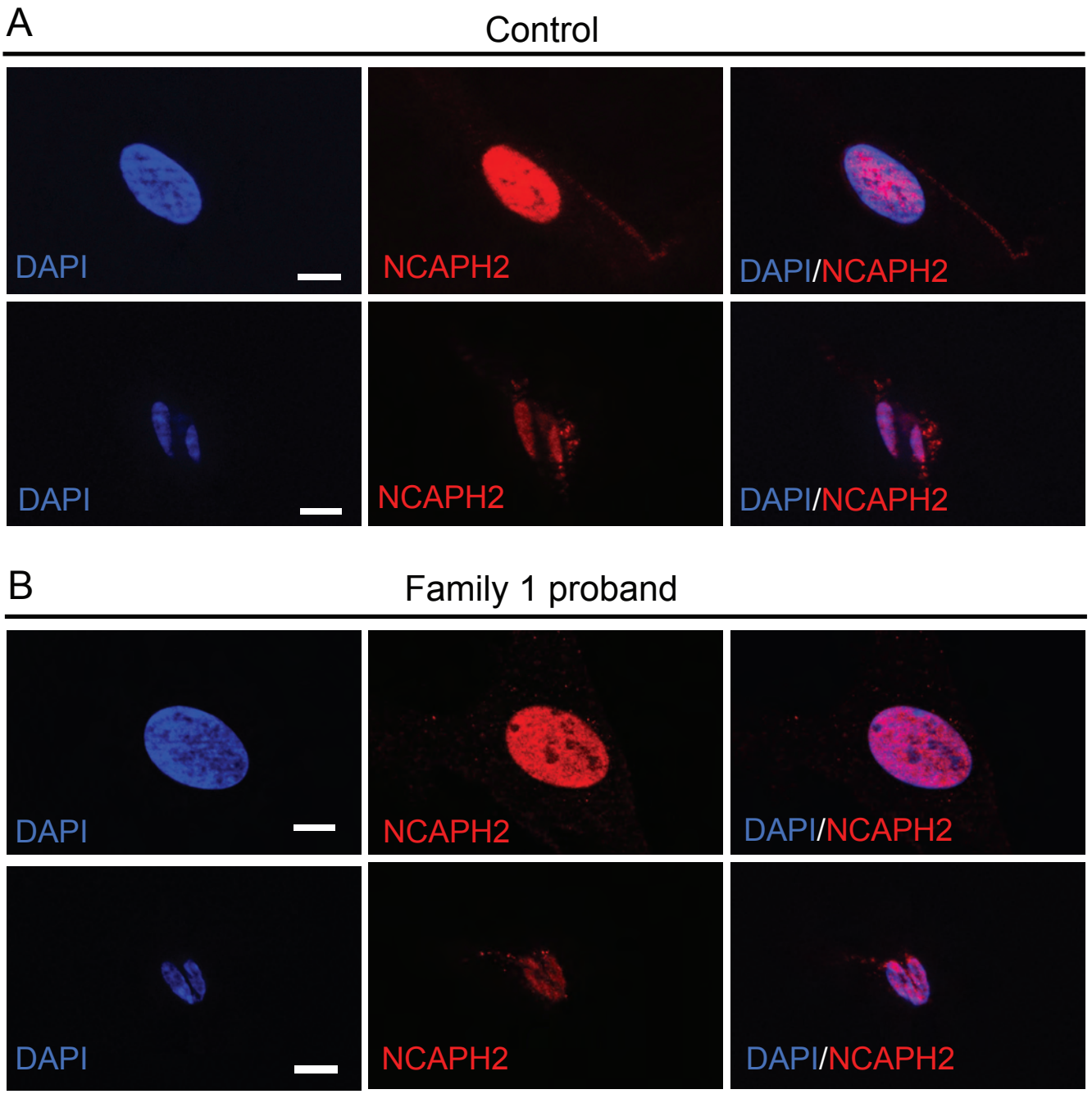
A
Control
DAPI
NCAPH2
DAPI/NCAPH2
DAPI
NCAPH2
DAPI/NCAPH2
B
Family 1 proband
DAPI
NCAPH2
DAPI/NCAPH2
DAPI
NCAPH2
DAPI/NCAPH2

Figure S3

Figure S3. NCAPH2 Immunofluorescence studies in family 1 proband primary fibroblasts shows no obvious cellular mislocalization.

(**A** and **B**) Representative epifluorescent images of control (**A**) and family 1 proband fibroblasts (**B**) were fixed and immunostained with anti-NCAPH2 antibody (Bethyl Laboratories; A302-276A-T, 1 μg/ml); nuclei were visualized with DAPI. NCAPH2 localizes to the nucleus in post-mitotic (top panels) and dividing cells (bottom panels). Scale bar, 10 μm; DAPI, blue, NCAPH2, red.

A

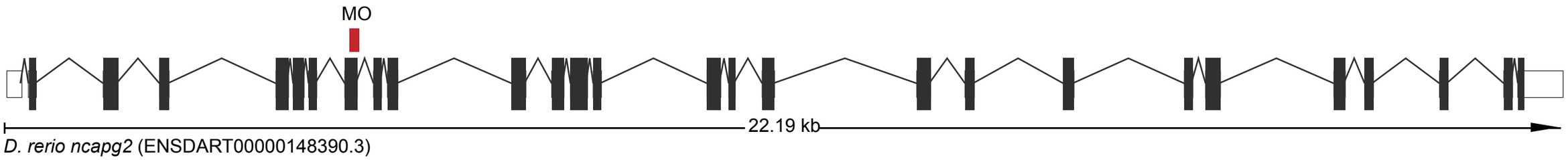

B

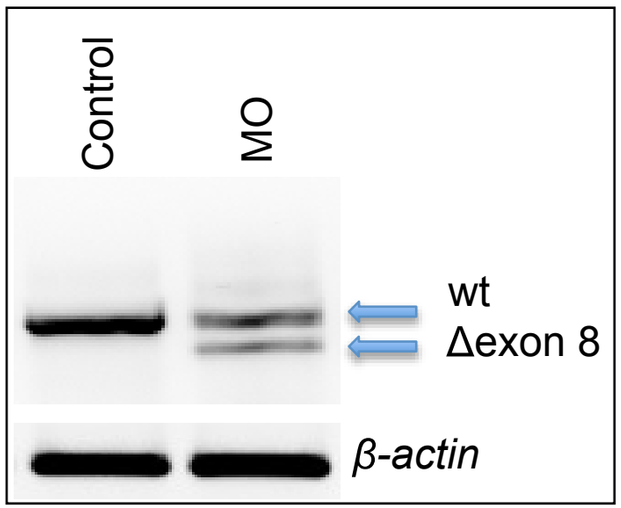

C

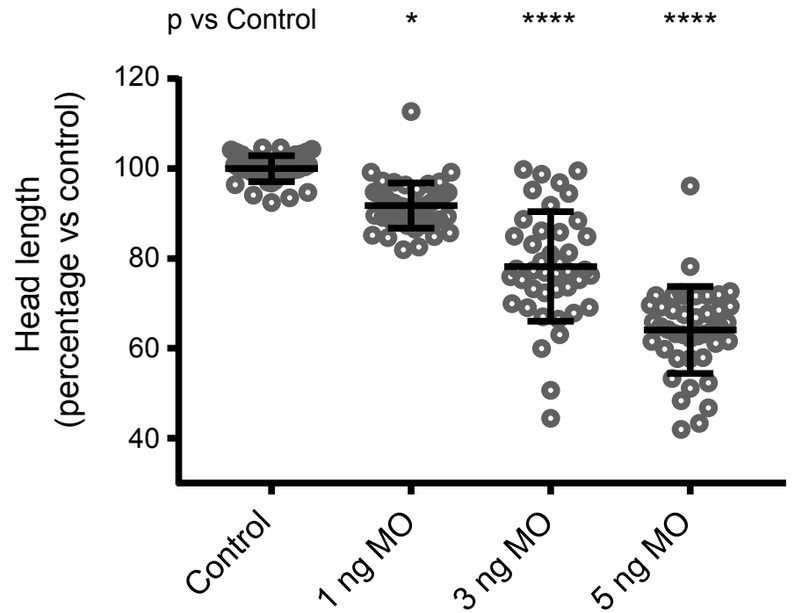

Figure S4

Figure S4. Validation of *ncapg2* transient suppression reagents in zebrafish.

(**A**) Schematic of *D. rerio ncapg2* (GRCz10); black boxes, coding exons; white boxes untranslated regions. The position of the splice blocking morpholino (MO; red box) target site at the exon 8 splice donor site is shown. (**B**) Agarose gel image indicates efficient targeting of the *ncapg2* MO. RT-PCR products were generated from control embryos and embryos injected with MO, and show a deletion of exon 8 (157 bp) resulting in a frameshift and premature termination codon in morphants. *β-actin* was used to control for RNA integrity. (**C**) Injection of MO results in a dose dependent effect on head size in zebrafish larvae that is significantly reduced compared to controls for all doses attempted. See Figure 3A for representative images and description of measurement. P-values were calculated using student's t-test; ; *, **** indicate $p<0.05$; and 0.0001 respectively; error bars represent standard deviation (s.d.); n=42-50 larvae/condition, repeated.

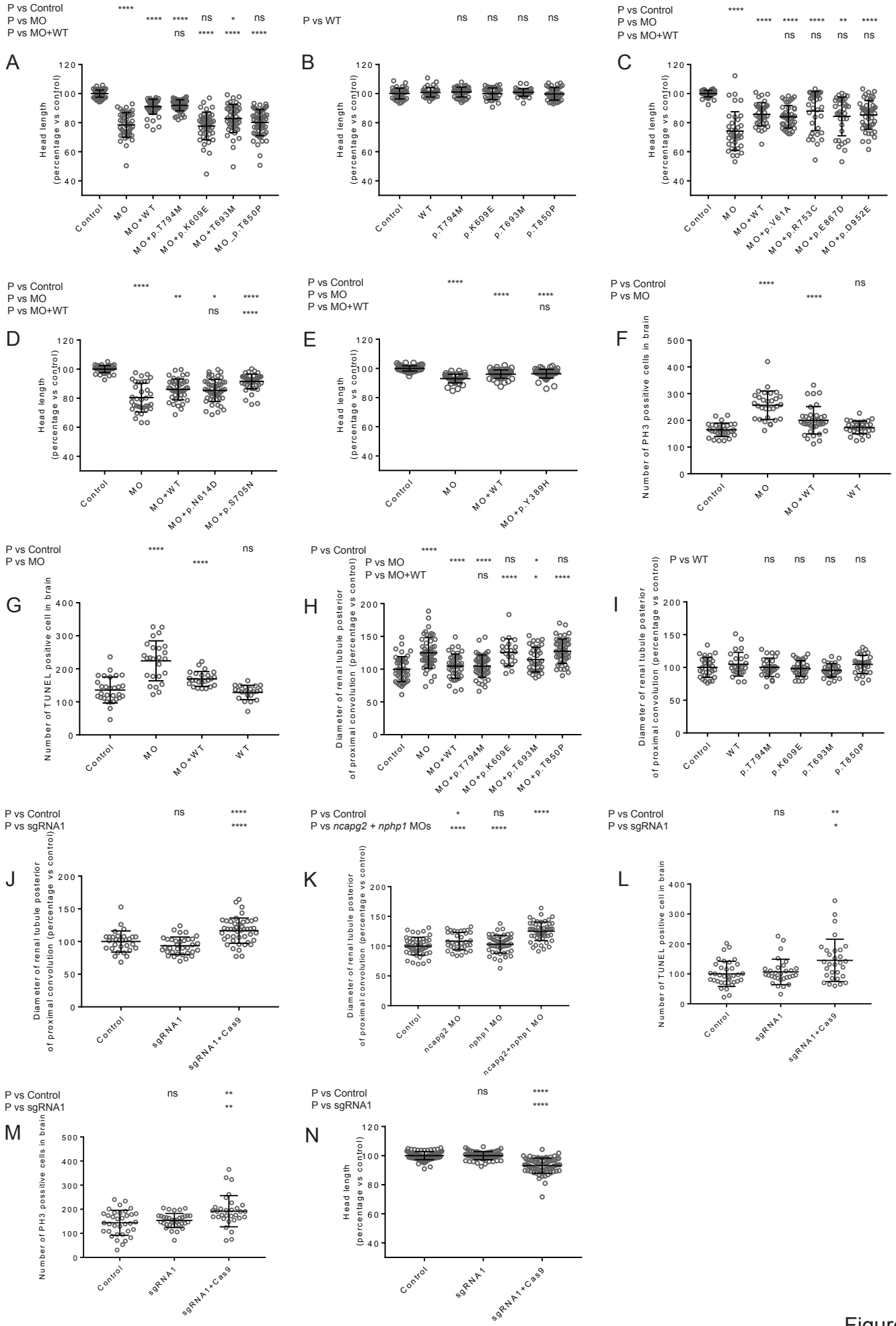
A
P vs Control
P vs MO
P vs MO+WT
Head length (percentage vs control)
Control
MO
MO+WT
MO+p.T794M
MO+p.K609E
MO+p.T693M
MO_p.T850P
B
P vs WT
Head length (percentage vs control)
Control
WT
p.T794M
p.K609E
p.T693M
p.T850P
C
P vs Control
P vs MO
P vs MO+WT
Head length (percentage vs control)
Control
MO
MO+WT
MO+p.V61A
MO+p.R753C
MO+p.E867D
MO+p.D952E
D
P vs Control
P vs MO
P vs MO+WT
Head length (percentage vs control)
Control
MO
MO+WT
MO+p.N614D
MO+p.S705N
E
P vs Control
P vs MO
P vs MO+WT
Head length (percentage vs control)
Control
MO
MO+WT
MO+p.Y389H
F
P vs Control
P vs MO
Number of PH3 possitive cells in brain
Control
MO
MO+WT
WT
G
P vs Control
P vs MO
Number of TUNEL positive cell in brain
Control
MO
MO+WT
WT
H
P vs Control
P vs MO
P vs MO+WT
Diameter of renal tubule posterior of proximal convolution (percentage vs control)
Control
MO
MO+WT
MO+p.T794M
MO+p.K609E
MO+p.T693M
MO+p.T850P
I
P vs WT
Diameter of renal tubule posterior of proximal convolution (percentage vs control)
Control
WT
p.T794M
p.K609E
p.T693M
p.T850P
J
P vs Control
P vs sgRNA1
Diameter of renal tubule posterior of proximal convolution (percentage vs control))
Control
sgRNA1
sgRNA1+Cas9
K
P vs Control
P vs ncapg2 + nphp1 MOs
Diameter of renal tubule posterior of proximal convolution (percentage vs control)
Control
ncapg2 MO
nphp1 MO
ncapg2+nphp1 MO
L
P vs Control
P vs sgRNA1
Number of TUNEL positive cell in brain
Control
sgRNA1
sgRNA1+Cas9
M
P vs Control
P vs sgRNA1
Number of PH3 possitive cells in brain
Control
sgRNA1
sgRNA1+Cas9
N
P vs Control
P vs sgRNA1
Head length (percentage vs control)
Control
sgRNA1
sgRNA1+Cas9

Figure S5

Figure S5. Dot plots of zebrafish phenotyping assays.

Dot plots were generated for each independent zebrafish experiment by inputting raw data into GraphPad. Statistical differences were calculated using a student's t-test; *, **, ***, **** indicate $p<0.05$; 0.01; 0.001; and 0.0001 respectively, ns indicates not significant. Error bars represent standard deviation. (**A, B** and **N**) correspond to Figure 3B, (**C-E**) corresponds to Figure S8, (**F** and **M**) correspond to Figure 4D, (**G** and **L**) correspond to Figure 4B, (**H-J**) correspond to Figure 3D, (**K**) corresponds to Figure 5B.

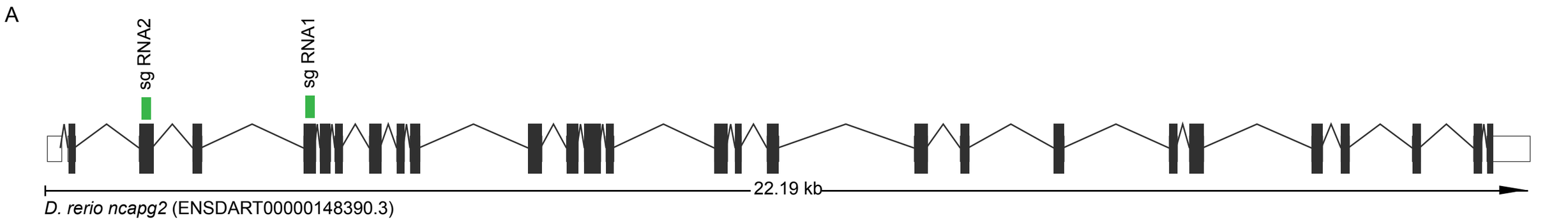
A
sg RNA2
sg RNA1
22.19 kb
D. rerio ncapg2 (ENSDART00000148390.3)
B
sgRNA1+Cas9 (F0)
Control
WT
ncapg2
C
sgRNA2+Cas9 (F0)
Control
WT
ncapg2
F
p vs Control
ns
****
Head length
(percentage vs control)
120
100
80
60
40
Control
sgRNA2
sgRNA2+Cas9
G
p vs Control
ns
****
Diameter of renal tubule posterior
of proximal convolution
(percentage vs control)
200
150
100
50
0
Control
sgRNA2
sgRNA2+Cas9
D
sgRNA1
PAM
Control
F0 mutatns
E
sgRNA2
PAM
Control
F0 mutatns

Figure S6

Figure S6. CRISPR/Cas9 genome editing of *ncapg2* in zebrafish embryos results in small insertion-deletions. (**A**) Schematic of *D. rerio ncapg2* (GRCz10); black boxes, coding exons; white boxes untranslated regions. The position of the single guide (sg)RNA target sequences are shown (green boxes) at exons 3 and 5. (**B** and **C**) Heteroduplex analysis of CRISPR/Cas9 F0 mutants. Embryos were harvested at 2 days post fertilization (dpf). We extracted genomic DNA and PCR-amplified a region flanking the sgRNA target site; PCR products were denatured, reannealed slowly, and migrated by polyacrylamide gel electrophoresis. CRISPR/Cas9 F0 mutant PCR products show heteroduplexes, indicating targeting events. (**D** and **E**) Representative chromatograms of cloned and sequenced PCR products derived from uninjected control embryos and F0 embryos injected with *ncapg2* sgRNA1 or sgRNA2 and CAS9 protein show insertion-deletion events in the target region; estimated mosaicism for sgRNA1 is 70% and sgRNA2 is 75% (n=3 F0 embryos per sgRNA, 24 clones each). The protospacer adjacent motif (PAM) sequence for each sgRNAs is denoted in blue. (**F**) *ncapg2* CRISPR/Cas9 F0 mutants (sgRNA2+Cas9) show a significant reduction in head size compared to controls or larvae injected with sgRNA2 alone (n=62-80 larvae/condition, repeated). See Figure 3A for representative images and description of measurement paradigm. (**G**) *ncapg2* CRISPR F0 mutants (sgRNA2+Cas9) show a significant increase in renal tubule diameter posterior of the proximal convolution compared to controls or larvae injected with sgRNA2 alone (n=33-37 larvae/condition, repeated). P-values were calculated using student's t-test; **** indicates $p<0.0001$; error bars, standard deviation (s.d.).

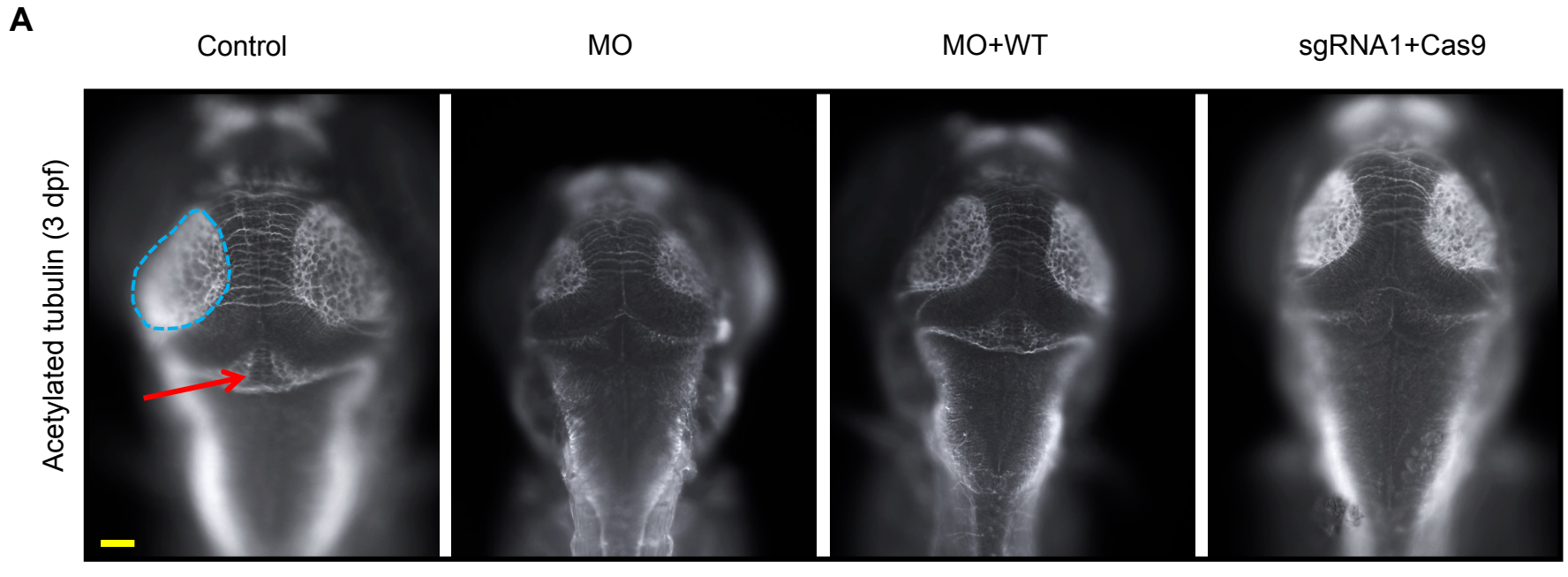
A
Control
MO
MO+WT
sgRNA1+Cas9
Acetylated tubulin (3 dpf)
B
p vs Control
ns
p vs MO
****
****
Size of optic tecta (percentage vs control)
150
100
50
0
Controls
MO
MO + WT
WT
C
p vs Control
ns
****
p vs sgRNA1
****
Size of optic tecta (percentage vs control)
150
100
50
0
Controls
sgRNA1
sgRNA1 + Cas9
D
p vs Control
****
ns
ns
**
p vs MO
****
Percentage of embryos
100%
80%
60%
40%
20%
0%
Control
MO
MO+WT
WT
sgRNA1
sgRNA1+Cas9

Figure S7

Figure S7. Suppression and CRISPR/Cas9 disruption of *ncapg2* results in central nervous system defects in zebrafish larvae. (**A**) Representative dorsal images of 3 dpf zebrafish larvae stained with acetylated tubulin antibody, showing a reduction in size of the optic tecta and cerebellar hypoplasia (blue dotted oval and red arrow, respectively) in morphants (MO) and CRISPR F0 mutants (sgRNA1+Cas9). Scale bar (yellow), 100 μm. (**B and C**) Quantification of the optic tecta size in morphants (MO) and F0 mutants (sgRNA1+Cas9) show a significant reduction compared to controls. Coinjection of MO with human WT *NCAPG2* mRNA (MO+WT) rescue optic tecta size significantly. n= 58-92 larvae/batch, repeated; statistical comparisons were performed with a student's t-test; error bars indicate standard deviation (s.d.). (**D**) Qualitative scoring indicates that a significant fraction of morphants (MO) and CRISPR F0 mutants display cerebellar abnormalities that can be rescued significantly by coinjection with human WT *NCAPG2* mRNA. n= 27-92 larvae/batch, repeated; statistical comparisons were performed using a Fisher's exact test. **, **** indicate $p<0.01$ and 0.0001 respectively ns, not significant in panels B, C and D.

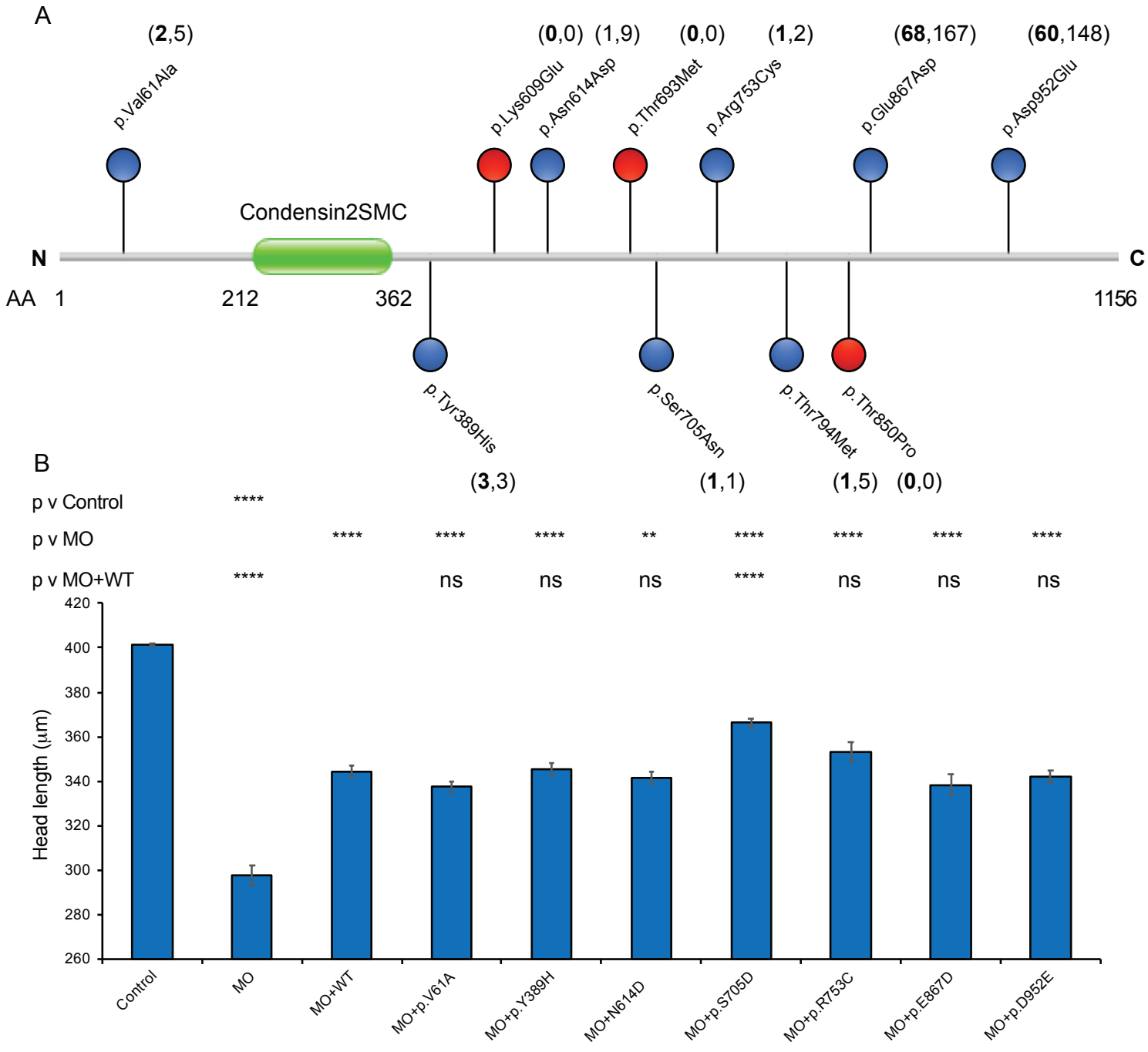
A
(2,5)
(0,0)
(1,9)
(0,0)
(1,2)
(68,167)
(60,148)
p.Val61Ala
p.Lys609Glu
p.Asn614Asp
p.Thr693Met
p.Arg753Cys
p.Glu867Asp
p.Asp952Glu
Condensin2SMC
N
C
AA 1
212
362
1156
p.Tyr389His
p.Ser705Asn
p.Thr794Met
p.Thr850Pro
B
(3,3)
(1,1)
(1,5)
(0,0)
p v Control
p v MO
p v MO+WT
Head length (μm)
Control
MO
MO+WT
MO+p.V61A
MO+p.Y389H
MO+N614D
MO+p.S705D
MO+p.R753C
MO+p.E867D
MO+p.D952E

Figure S8

Figure S8. *In vivo* complementation assays show that *NCAPG2* homozygous missense variants present in ExAC function similar to wild type.

In vivo complementation assays were performed in zebrafish using head size phenotyping. (**A**) Schematic showing homozygous *NCAPG2* variants found in ExAC. Control variants are represented with blue lollipops across the length of NCAPG2 protein (gray bar with green condensin2nSMC domain); red lollipops were identified in affected individuals reported in this study. Number of homozygotes present in ExAC and gnomAD are listed in parentheses for each variant; left bold integer, ExAC, right integer, gnomAD. Variant rs identifiers and ExAC MAFs are as follows: p.Val61Ala, rs187542564, MAF 0.002832; p.Tyr389His, rs61752309, MAF 0.003202; p.Asn614Asp, rs61740623, MAF 0.002469; p.Ser705Asn, rs115631698, MAF 0.001650; p.Arg753Cys, rs61745702, MAF 0.001649; p.Thr794Met, rs10248318, MAF 0.001784; p.Glu867Asp, rs3214000, MAF 0.01013; p.Asp952Glu, rs80143472, MAF 0.008845 (**B**) Quantitative analysis of head size using ImageJ to measure dorsal bright field images of 3 dpf zebrafish larvae. Statistical differences were calculated using student's t-test, n= 33-52, repeated; *, **, ***, **** indicate $p<0.05$; 0.01; 0.001; and 0.0001 respectively, ns indicates not significant. Error bars represent standard error of the mean (s.e.m.).

Supplementary Tables

Table S1: Condensin complex genes, associated human disorders and animal models

Human genes	Condensin system	Human disorder	Animal models		
			Mouse[Ψ]	Zebrafish[ε]	*Drosophila*[δ]
SMC2	Condensin I and II	na	Embryonic lethal	na	Increased mortality, neuroanatomical defects, partial lethality
SMC4	Condensin I and II	na	na	Reduced head size, neuroanatomical defects,	Reduced brain size, partial lethality
NCAPD2	Condensin I	Microcephaly (PMID: 27737959)	na	Reduced head size, decreased eye size, abnormal ploidy	Neuroanatomical defects, partial lethality
NCAPG	Condensin I	na	na	Decreased eye size, Retinal degeneration, Whole organism lethal	Abnormal variegation, lethality, increased mortality
NCAPH	Condensin I	Microcephaly (PMID: 27737959)	Embryonic lethal	Reduced head size, decreased eye size, abnormal ploidy	Lethality
NCAPD3	Condensin II	Microcephaly (PMID: 27737959)	na	na	Lethality
NCAPG2	Condensin II	na	Embryonic lethal	Reduced head size, neuroanatomical defects, renal tubule malformation*	na
NCAPH2	Condensin II	na	Reduced brain size, defective T cells, embryonic lethality	na	Infertility, partial lethality

[Ψ] http://www.informatics.jax.org/, [ε] http://zfin.org/, [δ] http://flybase.org/, *data from this study; na, not available.

Table S2: Whole exome sequencing capture statistics for family 1

Sample Name	% Total Reads Aligned	Avg Coverage	Reads Hit Target/ Buffer	% Targets Hit	% Base 1+ Coverage	% Base 10+ Coverage	% Base 20+ Coverage	% Base 40+ Coverage
Family 1 Father	98%	122	80%	99%	98.22%	96.19%	94.35%	87.66%
Family 1 Mother	97%	142	80%	99%	98.31%	96.56%	95.04%	89.96%
Family 1 Proband	97%	113	80%	99%	98.13%	96.03%	94.02%	86.28%
Average	97%	126	80%	99%	98.22%	96.26%	94.47%	87.97%

Table S3: Candidate variants in family 1 and family 2 subsequent to bioinformatic filtering.

Gene	Protein name	OMIM ID	Phenotype in OMIM	hg19 coordinate	Inheritance	Transcript (GenBank)	Nucleotide change	Protein change	Frequency in controls (gnomAD)*	PolyPhen-2	Mutation Taster
Family 1 (DM074)											
GLRA3	glycine receptor, alpha-3 subunit	600421	None	chr4:175710090	*de novo*	NM_006529.3	c.76G>A	p.Val26Ile	4/250022 (0.000016)	Benign	Disease causing
TTN	titin	604145; 613765; 608807; 603689; 611705; 600334	Cardiomyopathy, dilated, 1G; Cardiomyopathy, familial hypertrophic, 9 (AD); Muscular dystrophy, limb-girdle, type 2J (AR); Myopathy, proximal, with early respiratory muscle involvement; Salih myopathy (AR); Tibial muscular dystrophy, tardive (AD)	chr2:179474228	paternal	NM_133378.4	c.44105G>T	p.Ser14702Ile	(0.0004) 1 homozygote	Benign	Polymorphism
				chr2:179633490	maternal	NM_133378.4	c.9073C>G	p.Leu3025Val	(0.000004)	Probably damaging	Disease causing
NCAPG2	non-SMC condensin II complex subunit G2	608532	None	chr7:158455050	maternal	NM_017760.6	c.1825A>G	p.Lys609Glu	0	Benign	Polymorphism
				chr7:158449380	paternal	NM_017760.6	c.2078C>T	p.Thr693Met	7/245490 (0.00002851)	Probably damaging	Polymorphism
Family 2 (DM516)											
NCAPG2	non-SMC condensin II complex subunit G2	608532	None	chr7:158447908	maternal/ paternal	NM_017760.6	c.2548A>C	p.Thr850Pro	0	Probably damaging	Disease causing
CPZ	carboxypeptidase Z	603105	None	chr4:8609123	paternal	NM_003652.3	c.1165A>G	p.Lys389Glu	264/276878 (0.0009535)	Benign	Polymorphism
				chr4:8621112	maternal	NM_003652.3	c.1694G>A	p.Arg565His	113/277108 (0.0004078) 1 homozygote	Probably damaging	Disease causing
FAM184A	family with sequence similarity 184 member A	None	None	chr6:119399385	paternal	NM_024581.5	c.80G>T	p.Ala27Glu	112/176992 (0.0006328) 1 homozygote	Benign	Polymorphism
				chr6:119282948	maternal	NM_024581.5	c.3319A>G	p.Lys1107Glu	118/276832 (0.0004263 1 homozygote	Probably damaging	Disease causing

*Accessed January 2018

Table S4. Propidium iodide staining and flow cytometry revealed augmented G2/M arrest in the family 1 proband.

Control						**Family 1 proband (DM74-0001)**				
Marker	**Left**	**Right**	**Events**	**% Gated**		**Marker**	**Left**	**Right**	**Events**	**% Gated**
All	0	1023	9832	100.0		**All**	0	1023	9642	100.0
M1	201	348	9131	92.87		**M1**	201	348	8161	84.64
M2	348	515	282	2.87		**M2**	348	515	821	8.51
M3	515	695	430	4.37		**M3**	515	695	683	7.08

Table S5. *ncapg2* Morpholino and CRISPR sequences. Bold text indicates sequence complementary to target region.

	5'-3' sequence
ncapg2 MO	GATGTGTTTTCTGACCTGTCTGACT
ncapg2 sgRNA1_F	TAATACGACTCACTATAG**GGCGGGATTTACAAGGCA**
ncapg2 sgRNA1_R	TTCTAGCTCTAAAAC**TGCCTTGTAAATCCCGCC**
ncapg2 sgRNA2_F	TAATACGACTCACTATAG**GTGATCCAGCGCTCTGAAG**
ncapg2 sgRNA2_R	TTCTAGCTCTAAAAC**CTTCAGAGCGCTGGATCAC**

Table S6. Gene set enrichment analysis results generated from transcriptomic profiles of *ncapg2* F0 mutant vs *ncapg2* gRNA1-injected embryo heads at 2 dpf.

Name	Gene Ontology ID	Size	ES	NES	NOM p-val	FDR q-val	FWER p-val
Extracellular matrix structural constituent	GO:0005201	36	0.71	2.58	0	0.00E+00	0
Eye morphogenesis	GO:0048592	151	0.49	2.38	0	6.95E-04	0.001
Hindbrain development	GO:0030902	97	0.52	2.35	0	9.32E-04	0.002
Collagen trimer	GO:0005581	57	0.57	2.32	0	1.05E-03	0.003
Camera type eye morphogenesis	GO:0048593	114	0.51	2.31	0	8.43E-04	0.003
Lens development in camera type eye	GO:0002088	24	0.69	2.29	0	7.02E-04	0.003
Skeletal system development	GO:0001501	220	0.45	2.27	0	1.19E-03	0.006
Embryonic eye morphogenesis	GO:0048048	35	0.62	2.24	0	1.56E-03	0.009
Morphogenesis of a polarized epithelium	GO:0001738	19	0.70	2.21	0	1.39E-03	0.009
Sensory organ morphogenesis	GO:0090596	201	0.44	2.21	0	1.25E-03	0.009
Organ morphogenesis	GO:0009887	486	0.40	2.20	0	1.27E-03	0.01
Epithelial cell differentiation	GO:0030855	132	0.46	2.20	0	1.28E-03	0.011
Regulation of transmembrane receptor protein serine threonine kinase signaling pathway	GO:0090092	85	0.49	2.20	0	1.18E-03	0.011
Eye development	GO:0001654	280	0.42	2.19	0	1.30E-03	0.013
Camera type eye development	GO:0031076	229	0.43	2.19	0	1.31E-03	0.014
Non canonical Wnt signaling pathway	GO:0035567	31	0.63	2.18	0	1.58E-03	0.017
BMP signaling pathway	GO:0030510	73	0.51	2.16	0	2.15E-03	0.025
Pectoral fin development	GO:0033339	52	0.53	2.14	0	2.19E-03	0.027
Negative regulation of macromolecule biosynthetic process & Negative regulation of cellular macromolecule biosynthetic process	GO:0010558	157	0.44	2.14	0	2.22E-03	0.029
Negative regulation of biosynthetic process	GO:0009890	173	0.43	2.14	0	2.18E-03	0.03
Wnt signaling pathway	GO:0016055	167	0.43	2.13	0	2.68E-03	0.039
Negative regulation of cellular biosynthetic process	GO:0031327	172	0.43	2.13	0	2.68E-03	0.041
Ameboidal type cell migration	GO:0001667	148	0.44	2.12	0	2.69E-03	0.043
Regulation of transcription from RNA polymerase II promoter	GO:0006357	406	0.39	2.12	0	2.93E-03	0.049

Size, Number of genes in the gene set after filtering out those genes not in the expression dataset; ES, Enrichment score; NES, Normalized enrichment score; NOM p-val, statistical significance of the enrichment score; FDR q-val, false discovery rate; FWER p-val, Familywise-error rate.